Journal of Inorganic and Organometallic Polymers and Materials
https://doi.org/10.1007/s10904-024-03084-6

RESEARCH

# Polyvinyl Alcohol/Zr-based Metal Organic Framework Mixed-matrix Membranes Synthesis and Application for Hydrogen Separation

**Filiz Ugur Nigiz**[1,2] · **Tuba Ünügül**[2]

Received: 23 February 2024 / Accepted: 17 March 2024

## Abstract

Membrane gas separation is an environmentally friendly and economical method used to separate valuable gases, industrial process gas wastes, and carbon dioxide from mixed gases. The most important part of this method is the membranes. Gas separation membranes are expected to have high separation and permeability performance, high mechanical strength, easy and fast production capability, and low prices. Polymer-based membranes are mostly preferred depending on the ease of modification capability. In this study, a zirconium-based metal organic framework (Zr-MOF, MIL-140 A) was synthesized and used as a filler within polyvinyl alcohol (PVA) matrix for the selective separation of hydrogen ($H_2$) from carbon dioxide ($CO_2$). The effect of MIL-140 A addition on the mechanical, structural, and morphological properties of PVA was evaluated. The MIL-140 A significantly improved the mechanical strength of the membrane. According to the gas separation results, the increasing concentration of MIL-140 A increased the selective separation performance of the nanocomposite membrane. The highest mechanical strength (43.1 MPa) and best film-forming ability were obtained with 3 wt% MIL-140 A loaded membrane. The ideal $H_2/CO_2$ selectivity and hydrogen permeability were obtained as 5.6 and 944 Barrer, respectively at 2 bar feed pressure and room temperature. The highest ideal $H_2/CO_2$ selectivity was obtained as 6.3 with the H2 permeability of 959 Barrer when the MIL-140 A ratio was 4 wt%.

**Keywords** Hydrogen separation · Membrane gas separation · Zirconium based MOF · Polyvinyl alcohol membrane

## Abbreviations

| | |
|---|---|
| BET | Brunauer-Emmett-Teller |
| BN | Boron nitride |
| COF | Covalent organic framework |
| DSC | Differential scanning calorimeter |
| EPDM | Ethylene propylene diene monomer |
| FTIR | Fourier transform infrared spectroscopy |
| GO | Graphene oxide |
| IL | Ionic liquid |
| LDH | Layered double hydroxide |
| MOF | Metal organic framework |
| PA | Polyamide |
| PBI | Polybenzimidazole |
| PC | Polycarbonate |
| PDMS | Polydimethyl siloxane |
| PEBA | Polyether block amide |
| PI | Polyimide |
| PSA | Pressure swing adsorption |
| PU | Polyurethane |
| PVA | Polyvinyl alcohol |
| PVC | Polyvinyl chloride |
| PVDF | Polyvinylidene fluoride |
| SBR | Styrene-butadiene rubber |
| SEM | Scanning electron microscopy |
| TFN | Thin Film Nanocomposite |
| TGA | Thermogravimetric analysis |
| Zr | Zirconium |

## Symbols

| | |
|---|---|
| A | Effective membrane area ($cm^2$) |
| l | Membrane thickness (mm) |
| Q | Volumetric flow rate ($cm^3/s$) |

---

✉ Filiz Ugur Nigiz
filiz.ugur@comu.edu.tr

Tuba Ünügül
unugultuba@gmail.com

[1] Chemical Engineering Department, Çanakkale Onsekiz Mart University, Çanakkale 17020, Turkey

[2] Chemical Engineering Department, Kocaeli University, Kocaeli 41380, Turkey

| | |
|---|---|
| Δp | Pressure difference or transmembrane pressure (cmHg) |
| t | Operation time (h) |
| p | Permeability (Barrer) |
| α | Ideal Selectivity |
| Tm | Melting Temperature |
| ΔHm | Melting entalphy |

## 1 Introduction

Membrane gas separation method, which is an alternative to traditional purification methods, has many advantages such as ease of installation, low operation consumption, and low energy cost [1–4]. The process of gas separation employs several membrane types, including polymeric, inorganic, composite, and mixed-matrix membranes. Polymeric membranes have a number of benefits, including ease of use, reusability, affordability, and exceptional mechanical qualities [5–8].

There are many polymeric membranes used in membrane gas separation studies. It is possible to categorize them according to their different characteristics. According to the structural mobility, polymeric membranes can be divided into two groups as rubbery and glassy. While glassy polymers are more rigid and have high diffusion selectivity, rubbery polymers have high permeability. Polyvinyl alcohol (PVA), polyimide (PI), polyethersulfone (PES), polysulfone (PSF), polyamide (PA), polycarbonate (PC), polyvinyl chloride (PVC) are the most known gas separation membrane material that is categorized as glassy polymers [9–12]. Styrene-butadiene rubber, polyetherblockamide (PEBA), polydimethylsiloxane (PDMS), ethylene propylene diene monomer (EPDM), polyurethane (PU) poly(vinylidene fluoride)(PVDF) [13–15] are the most known rubbery state polymeric materials. The chain mobility of rubbery membranes is intense under normal conditions. Meanwhile, the intermolecular spaces (void spaces) are generally quite wide. This ensures high permeability in gas separation processes. They are especially used in the separation of large diameter gas molecules based on their solubility rather than their molecular size. However, selectivity values are generally low, especially if the kinetic diameter of the gas to be separated is considerably smaller than other gases (for example, to separate nitrogen from methane). This situation can be overcome by making some chemical and physical modifications. On the other hand, glassy polymers have more rigid structures depending on the glass transition temperature. Unlike rubbery polymers, chain movements are restricted below the glass transition temperature. This allows lower gas permeability values [9]. It increases the separation performance by increasing diffusion selectivity, especially in gas separation process that occurs according to the molecular size.

Polyvinyl alcohol (PVA) is produced by the hydrolysis reaction of polyvinyl acetate [16]. It is widely preferred in various industrial application areas, such as pharmaceuticals, packaging, and membranes. Oil-water separation [17], pervaporation [18], air filtration [19], and gas separation are the most preferred membrane-based technologies for the use of PVA membrane depending on the water-soluble, non-toxic, high chemical, and mechanical resistance properties. PVA is recommended in many membrane gas separation applications owing to its modification characteristics [20, 21]. Modifications made to the PVA membrane directly increase gas separation performance. Xu et al. (2023) prepared a graphene oxide (GO) loaded PVA membrane for the selective separation of $CO_2$ from $H_2$. They reported that the $CO_2/H_2$ selectivity significantly increased from 10 to 22 with the incorporation of GO [22]. Klepic et al. (2020) examined the gas separation performance of PVA/ionic liquid-loaded membranes. They reported that the $H_2/CO_2$ selectivity increased with the addition of ionic liquid [23]. Wong et al. (2021) investigated the gas separation performance of PVA/PEBAX (polyether bloc amide) membranes with different blend ratios. They obtained the highest permeability of 20 Barrer and the $CO_2/H_2$ selectivity of 7.6 with 60 wt% PEBAX/40 wt% PVA membrane [24]. There are many polymer-based gas separation membranes in the literature. These generally have low selectivity. It is possible to increase their selectivity by making some improvements without permeability loss. Blending, cross-linking, grafting, and liquid or nanofiller addition are well-known modification techniques. Adding functional nanoparticles not only increases the physical, chemical, and thermal resistance of the membrane but also significantly improves the separation performance. Materials such as metal organic frameworks (MOF), zeolite imidazole frameworks (ZIF), covalent organic frameworks (COF), graphene, borophene are known to increase all the properties of the membrane simultaneously. These materials can also be synthesized alone as membranes. However, the production process is long, and quite expensive, and the materials require support. Therefore, high-performance gas separation results are achieved by adding these smart particles into polymeric membranes and making them mixed matrix membranes (MMM).

There are many studies using mixed matrix polymeric membranes with the addition of fillers to increase the selectivity of the membranes [25]. Xing and Ho (2011) prepared fumed silica (FS) loaded PVA membranes for $CO_2/H_2$ separation. They used a mixture of gas of 20% $CO_2$ and 80% $H_2$. They reported that the $CO_2/H_2$ selectivity increased with the cross-linking degree of PVA. They reported that when the silica ratio was increased from 12 wt% to 22 wt%, the $CO_2$/

$H_2$ selectivity increased from 65 to 87%, but the $CO_2$ permeability remained constant as 1130 Barrer [26]. Ahmad et al. (2013) prepared mixed matrix membranes including different ratios of $TiO_2$-loaded PVA membranes. They reported that they obtained the highest $H_2/CO_2$ selectivity of 1.15 with 30 wt% of $TiO_2$ loaded membrane [27]. Kheirtalab et al. (2020) studied the $CO_2/CH_4$ separation performance by preparing GO (2-4-6 wt%) loaded PVA membranes. They reported that the permeability and $CO_2/CH_4$ selectivity increased depending on the graphene oxide ratio [28]. Li et al. (2021) prepared GO, boron nitride (BN), and molybdenum disulfide (MS) incorporated PVA membranes [29]. They found that the permeability value increased from 36.8 Barrer to 144 Barrer by the addition of 1 wt% GO into the pristine PVA membrane. They also reported that the 102.5 $H_2/CO_2$ selectivity was obtained with the addition of 2 wt% BN and this value was above the Robeson upper bond.

Metal organic frameworks (MOFs) are organic-inorganic nanomaterials that contain positively charged metal ions. They have numerous advantages, such as high surface area, porosity, strong mechanical stability, and high thermal stability [30–32]. It is useful in numerous application fields, including catalysis, gas separation, adsorption, and hydrogen storage [33–36]. MIL-coded MOF is a kind of zirconium form MOF that has a triangular cage structure with short linkages. It is resistant to corrosion, chemicals, and water. MIL-140 A is one of the MIL's family which has the narrowest pore diameter [34, 37]. Their adjustable pore diameters make them particularly suitable materials for gas separation. However, there are very limited studies on the use of MOFs for gas separation. Ozen and Ozturk (2019) prepared polyimide (PI)-based Co, Cu, and Ni MOFs and studied the effect of MOF types and ratios on gas separation. They reported that gas permeability increased in parallel with the MOF addition into MMM. The highest gas permeability and $H_2/CO_2$, $H_2/CH_4$, and $CO_2/CH_4$ selectivity were obtained using Cu-MOF based MMM. The hydrogen, carbon dioxide, and methane permeability increased to 62.86%, 94.00%, and 121.27%, respectively by using 5 wt% Cu-doped MOF-5-polyimide membrane compared to the pristine membrane [38]. Ashtiani et al. (2021) studied the effect of UiO-66-$NH_2$ (3, 8, 13, 24, 55 wt% in PVA) on $CO_2/N_2$ gas separation performance. They reported that the permeability of $CO_2$ was higher than that of $N_2$ at all MOF ratios and the permeability value increased as the MOF ratio increased for both gases. The highest $CO_2/N_2$ selectivity was obtained with 24 wt% MOF incorporated membrane. However, the $CO_2/N_2$ selectivity values for all MOF ratios remained below the Robeson upper limit value [39]. MIL-140 A was previously studied for gas adsorption and promising adsorption results were obtained [37, 40, 41]. Prakash et al. (2015) reported in their study that MIL-140 A-based mixed matrix membranes could potentially be used for $H_2/CO_2$ separation [40].

In this study, MIL-140 A was synthesized and used as filler in polyvinyl alcohol membrane at different concentration. The morphological, chemical, thermal, and mechanical performance of the pristine and nanocomposite membranes were investigated. Effect of MIL-140 A ratio on the separation performance of $H_2/CO_2$ gas separation were performed. According to the authors' knowledge, PVA/MIL-140 A membranes were synthesized and used for $H_2/CO_2$ for the first time in the literature.

## 2 Materials and Methods

### 2.1 Materials

Polyvinyl alcohol (Mowiol, MW: 125,000, 98.0–98.8 mol% hydrolysis), terephthalic acid (98% purity), and zirconium chloride (≥ 99.5% purity) were purchased from Aldrich Chemicals, Turkey. Acetic acid (≥ 99%, analytical grade), N,N-dimethylformamide (DMF), and methanol (anhydrous, 99.8%) were purchased from Merck Chemicals.

### 2.2 Methods

#### 2.2.1 MIL-140 a Synthesis

MIL-140 A was synthesized according to the solvothermal method which was also prepared in the previous study [42]. The procedure was modified from the study of Yahaya et al. (2022) [43]. 0.03 mol of zirconium chloride, 0.06 mol of terephthalic acid, 35 ml of DMF, and 0.32 ml of acetic acid were mixed and stirred at 220 °C for 24 h. The solution was then allowed to cool at room temperature and washed with methanol several times. Then, the particles were stirred with methanol overnight and filtrated to obtain MIL-140 A particles. The produced MIL-140 A particles were dried in an oven at 80 °C for 12 h.

#### 2.2.2 Membrane Preparation

Pristine PVA and mixed-matrix membranes were prepared by mixing 10 wt% PVA aqueous solution at 80°C for 5 h. Separately, MIL-140 A was dissolved in water and distributed for 15 min in an ultrasound bath. Then, MIL-140 A/water solution was added to the PVA solution and mixed for 2 h at room temperature with a stirring speed of 500 rpm. 0.1 wt% glycerol was added to the solution to prevent the membrane from adhering to the glass surface. Then the solution was poured onto the glass plate and left to dry at room temperature with the humidity above 50%. The ratio

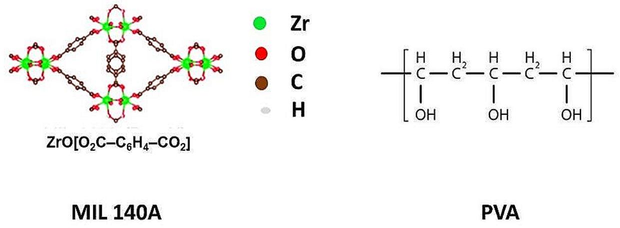

**Fig. 1** Molecular and chemical structure of MIL-140 A and PVA

of MIL-140 A in mixed matrix membranes was determined as 1-2-3-4 wt%, based on the weight of PVA. Membranes were coded with the name of the polymer and the ratio of the MIL-140 A. No cross-linking or thermal treatment was applied to the prepared membranes. The final thickness of the membranes was measured as 33 ± 2 µm. The schematic representation of MIL-140 A and PVA structure is given in Fig. 1. Due to the strong physical-chemical bonding ability of the hydroxyl groups in PVA and hydrogen in MIL-140 A, it appears that the mixed matrix membrane can be suitable for gas separation.

### 2.2.3 Characterization

The structure of the MIL-140 A material and the cross-sectional morphologies were analyzed using scanning electron microscopy (JEOL JSM-7100-F). SEM analysis was conducted at 10 kV and 30 kV for the PVA membranes and MIL-140 A, respectively.

The X-ray diffraction (XRD) test was used to determine the crystalline-amorphous structures of MIL-140 A, PVA, and MMM using a PANalytical EMPYREAN XRD device. The test was conducted in the 5°–70° range.

The functional groups of MMMs, the state of their structural bonds, and their binding sites were determined using Perkin Elmer Spectrum Fourier transform infrared spectroscopy (FTIR). The experiment was conducted in the 4000–650 $cm^{-1}$ wavelength range.

Thermal gravimetric analysis (TGA, Mettler Toledo TGA Instrument) was done to investigate the thermal behavior of membranes. The heating rate was 10 °C/min. The test was done from 25 °C to 600 °C under the nitrogen gas atmosphere.

The melting enthalpy ($\Delta H_m$), glass transition temperature ($T_g$), and melting temperature ($T_m$) of the filled and unfilled membranes were evaluated using the differential scanning calorimeter (DSC, Mettler Toledo). The temperature of the membrane samples was increased from 25 °C to 250 °C with the temperature step of 10 °C/minute.

The universal testing device (ANKARIN) was used for the mechanical tests. ASTM D882 standard was used to determine the mechanical character. Membranes were divided into strips (40 mm long and 10 mm wide). They were stretched at a crosshead rate of 10 mm/minute.

## 2.3 Gas Permeation Set-up

A constant pressure gas permeation performance for single $H_2$ and $CO_2$ was carried out in membrane gas permeation system which is illustrated in Fig. 2. The system consists of a stainless-steel membrane cell, where the gas permeation is carried out by placing the membranes, the pressure control device, and a digital flow meter (Omega, 13–100 mL/min, %3 accuracy) to ensure that the gases are at the specified constant pressure and flow rate. The active separation area of the membrane was 7 $cm^2$.

The performance of separation is determined depending on the single gas permeability (P) and ideal gas selectivity (α) (Eqs. (1 and 2) in which is described elsewhere [44]

**Fig. 2** Single gas separation test unit

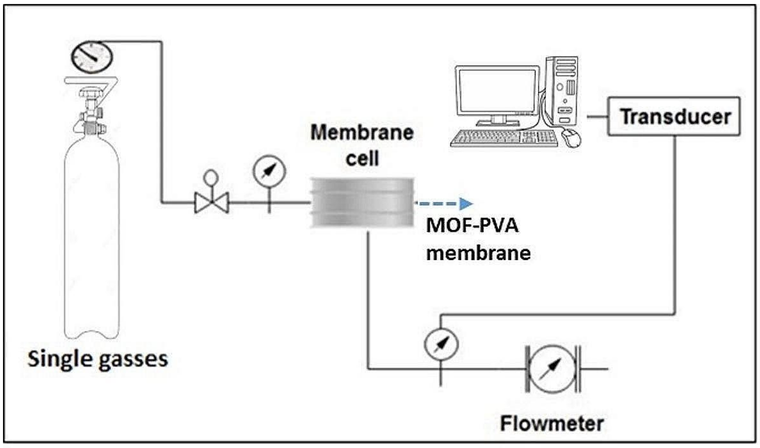

$$P = \frac{Ql}{A\Delta P} \tag{1}$$

$$\alpha_{H_2/CO_2} = \frac{P_{H_2}}{P_{CO_2}} \tag{2}$$

## 3 Results and Discussions

### 3.1 Characterization Results

In the gas separation process, the membrane must have two important features other than gas separation performance. The first is its non-porous structure and the second is its mechanical strength. It is important to determine these properties before performing gas permeability tests of the membrane. Figure 3 shows the SEM analysis of MIL140A, pristine, and MIL-140 A-loaded PVA membranes. As indicated in Fig. 3a, the sizes of the MILs were almost homogeneous and there were crystal structures that could not be synthesized, but they were very few.

Gas separation is a molecular-level separation process. The most known problem that can be encountered, especially when preparing nanocomposite materials containing fillers, is the properly distribution of fillers through the membrane. Moreover, the adhesion between polymer and filler must be strong. Therefore, SEM analysis is critical for membrane characterization. Figure 3b and c show the homogeneous distribution of MIL-140 A material on the PVA surface. The point and lighter-colored phases visible in the membrane represent MIL-140 A materials. As can be seen, the distribution of the particles onto the surface is homogeneous. Figure 3d shows both the surface and cross-sectional view. The thickness of the membrane was about 33 µm. As seen in Fig. 3c and d, the membrane was synthesized as smooth, non-porous, and quite regular. However, some MIL-140 A particles also appear to be agglomerated. This is due to the high interaction between MIL-140 A particles. Moreover, the surface repulsive forces between the polymer and MIL-140 A structures can be effective. Although an ultrasonic bath is used to separate MIL-140 A particles through the polymer matrix, aggregations are observed in some places.

Figure 3de 3f, 3 g, and 3f h show the cross-sectional SEM images of the membranes at different MOF loading. As can be seen, as the MOF ratio increases, the amount of particles accumulated in the cross-section also increases. It is also observed that particles aggregate at higher loading rates (Fig. 3h). However, it is necessary to evaluate these results together with the mechanical analysis and separation results to determine its positive-negative effect.

Since gas separation is a pressure-driven process, the mechanical strength of the membrane is as important as the separation performance. Even if the membrane separation is perfect, a membrane that cannot withstand pressure cannot be commercialized. Therefore, the mechanical strength and separation results should be evaluated together to determine the appropriate concentration for filler. Mechanical analysis tests were carried out on a tensile test device according to ASTM D882 standard. The percentage of elongation at break (%) and tensile stress at maximum load values were calculated. Figure 4 shows the mechanical test results of

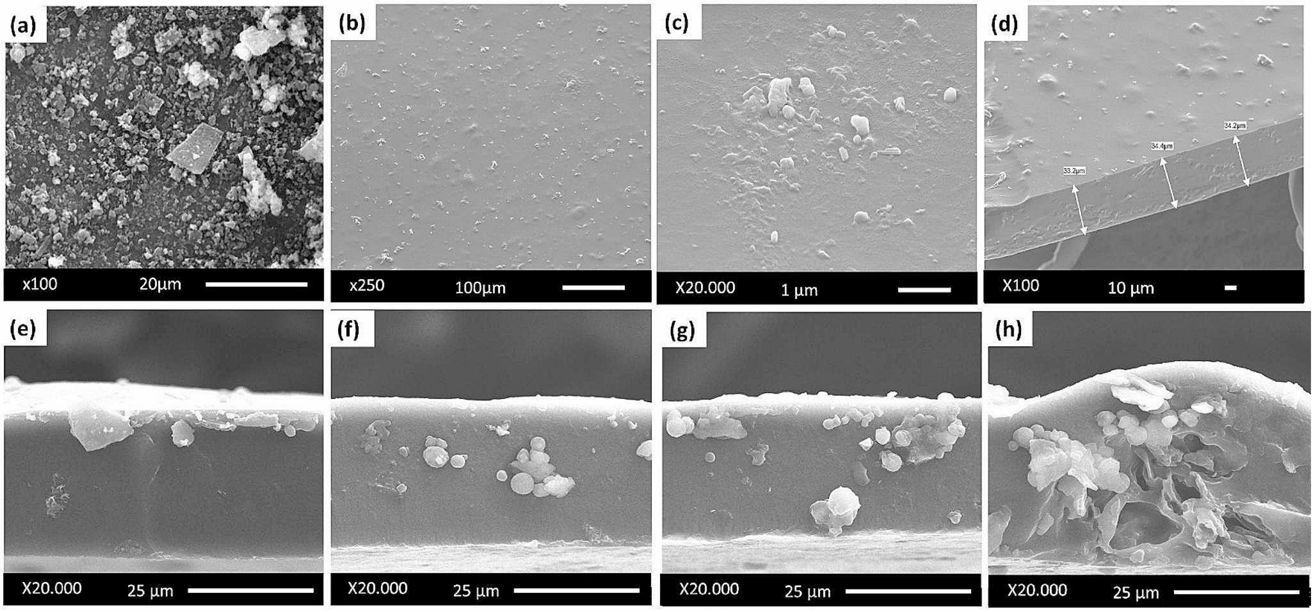

**Fig. 3** Surface SEM analysis of MIL-140 A (**a**), 3 wt% MIL-140 A loaded MMM (**b**, **c**, an **d**) and cross-sectional view of PVA-1 wt% MIL-140 A(e), PVA-2 wt% MIL-140 A (**f**), PVA-3 wt% MIL-140 A (**g**), and PVA-4 wt% MIL-140 A (**h**) loaded membranes

the pristine and MIL-140 A-loaded PVA membranes. The tensile strength values of the membrane increased from 23.7 MPa to 43.1 MPa with the increase of fillers from zero to 3 wt%. In other words, there is a significant improvement in mechanical strength due to the increase in MIL-140 A concentration. This can be attributed to the improved interfacial interaction between the nanofillers and the polymeric matrix [45–47]. In addition, the homogeneous dispersion of the nanofiller into the polymer matrix leads to the formation of homogeneous phase morphology. However, a decrease in tensile from 43.1 MPa to 26.4 MPa was observed after the MIL-140 A ratio exceeded 3 wt%. This situation can correspond to the excess filler loading rate which was also indicated in Fig. 3h (SEM analysis). The polymer-filler interaction may be weak due to the agglomeration of fillers.

Mechanical analysis is a very important performance parameter for membranes that will operate at high pressure. Therefore, it can be seen that this value for PVA decreases after 3 wt% MIL-140 A loading. For this reason, gas separation studies were carried out until the point where the mechanical strength decreased. Characterization tests were also carried out for the pristine and 3 wt% MIL-140 A loaded membranes, so the difference can be seen more clearly.

FTIR is an analysis that shows the interaction of additives with the matrix. In this study, the ratio of additives (MIL-140 A) was changed between 1 and 4 wt%. There is no significant chemical change is expected in the FTIR samples. Only the physical interaction such as water retention can be observed. As the MIL ratio increased, the bond structure it affected gradually increased. For this reason, only the effect of MIL-140 A contribution (3 wt%) has been examined to better understand the analysis and avoid confusion. The FTIR spectra of the pristine and 3 wt% MIL-140 A loaded PVA membrane is given in Fig. 5.

There are some important findings seen in the spectra. One of them is that the ratio of the -OH stretching vibration peak seen at 3280 cm$^{-1}$ points depending on the water-moisture content decreased as the MIL-140 A addition. Considering the density and membrane hydrophilicity of the -OH peaks in PVA, MIL-140 A has less water holding capacity and moisture content than PVA. Peaks in the –$CH_3$ bond in membranes vary between 2998 cm$^{1}$ and 2880 cm$^{-1}$. The peaks observed at 1420 cm$^{-1}$ and 1510 cm$^{-1}$ belong to C = C in the aromatic compound of the organic binder. The peaks around 1600 cm$^{-1}$ can be said to be DMF residues used in the synthesis of MOF material. While the bands at 830 and 740 cm$^{−1}$ are the result of aromatic C–H bending vibrations, the bands at 1150 and 1023 cm$^{−1}$ may be attributed to C–H bending vibrations in terephthalates [48].

XRD patterns of the MIL-140 A, the pristine PVA membrane, and 3 wt% MIL-140 A loaded PVA membrane is shown in Fig. 6. The primary distinctive peaks of Zr-based MOF materials are seen at $2\theta = 7.43$ and 8.75° as shown in Fig. 6 (red graphs). Other peaks are related to the noise and the majority of contaminants. It is seen that the MIL-140 A structure is entirely crystalline. The XRD pattern of the MOF particle is similar to other research in the literature [48, 49].

The blue line shows the pristine PVA membrane which has a large diffraction peak at $2\theta = 20^\circ$ indicating the semi-crystalline structure. As can be seen from the black graph, the degree of amorphous groups is increased in the PVA membrane by MIL-140 A incorporation.

**Fig. 4** Effect of MIL-140 A rate on stress and strain values

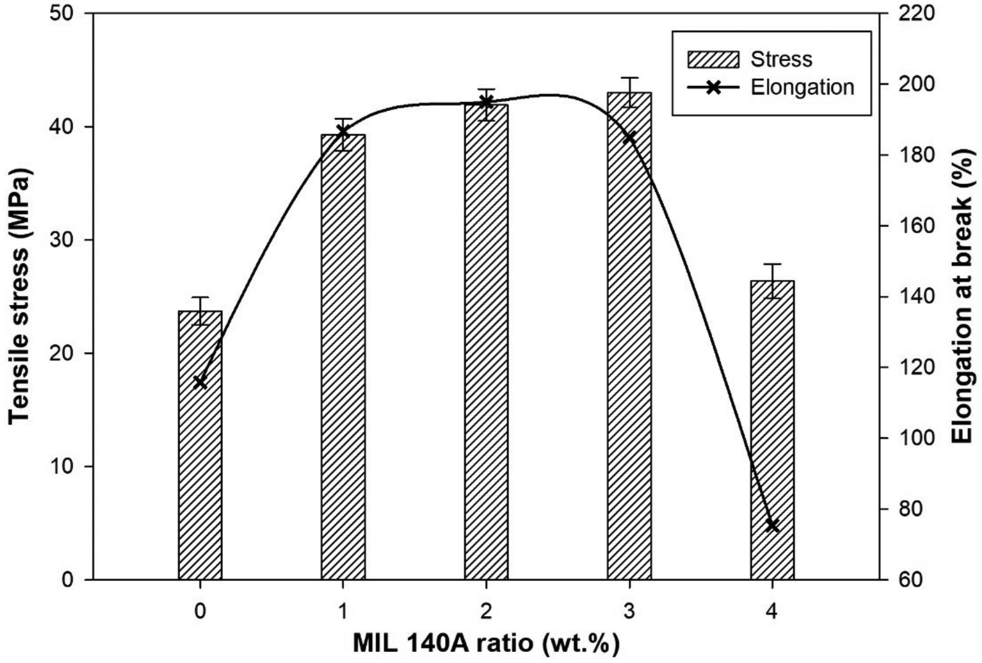

**Fig. 5** FTIR spectrum of the unfilled and 3 wt% MIL-140 A filled PVA

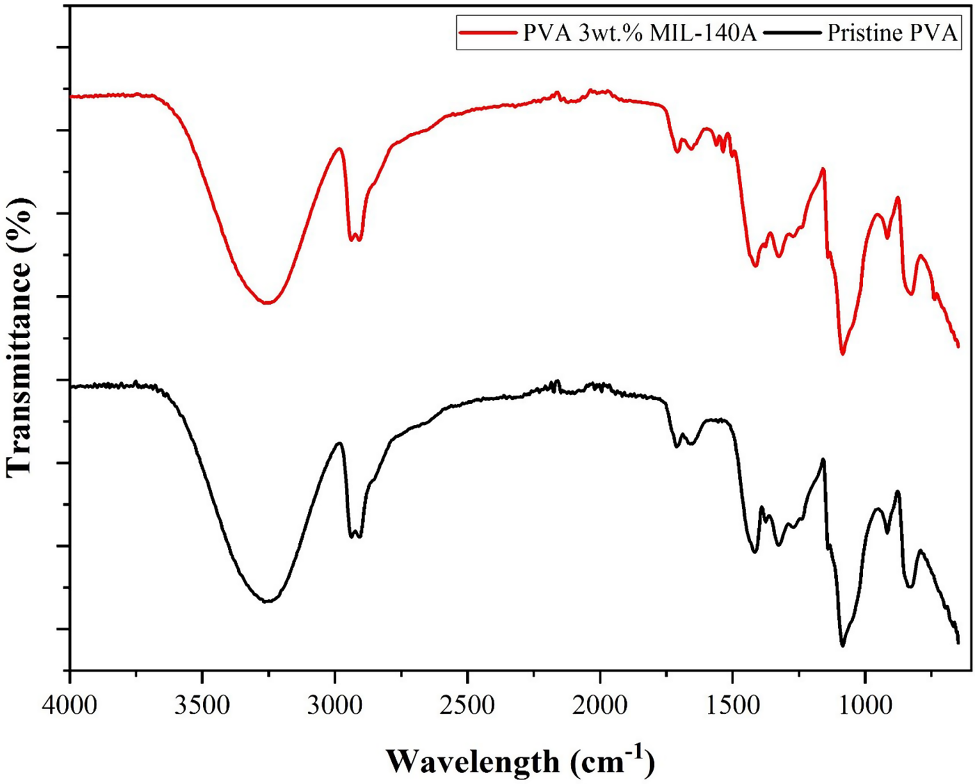

**Fig. 6** XRD patterns of the pristine, 3 wt% MIL-140 A loaded membrane and MIL-140 A particle

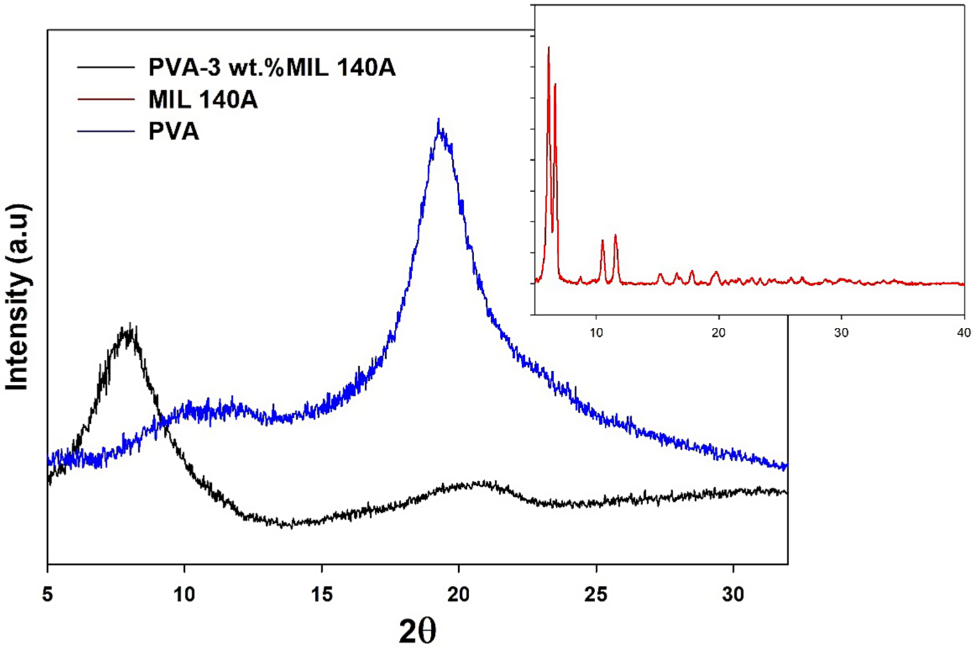

TGA experiments were evaluated to determine the thermal properties of membranes. TGA and DTGA thermograms of the pristine and 3 wt% MIL-140 A loaded membranes are given in Fig. 7a and b, respectively. The characteristic thermal properties of $T_5$ (the temperature that lost 5 wt% of the polymer mass), $T_{10}$ (the temperature that lost 10 wt% of the polymer mass), and $T_{max}$ (the maximum temperature at which decomposition occurs) are given in the figures.

As represented in Fig. 7; Table 1, the pristine PVA membrane had three degradation steps while the PVA $-3$ wt% MIL-140 A membrane showed four degradation steps. The first decomposition temperature, which occurs between 105-110°C, is due to the single-crystal structure of the MOF

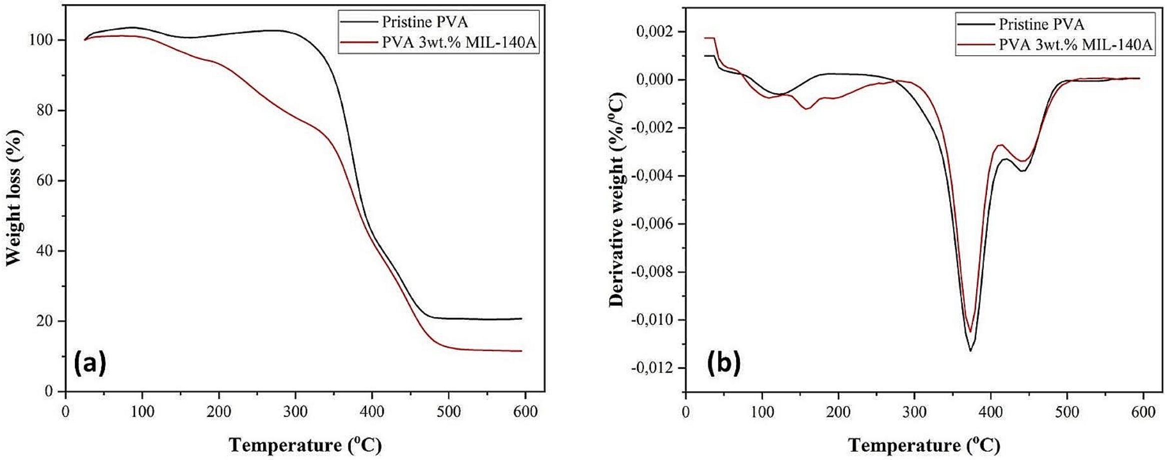

**Fig. 7** TGA of the membranes **a** TGA **b** DTGA

**Table 1** Thermal property of membranes

| Samples | $T_{max-1}$ (°C) | $T_{max-2}$ (°C) | $T_{max-3}$ (°C) | $T_{max-4}$ (°C) | $T_5$ (°C) | $T_{10}$ (°C) | Ash (wt%) |
|---|---|---|---|---|---|---|---|
| Pristine PVA | - | 121.88 | 373.52 | 441.89 | 337.45 | 349.20 | 20.75 |
| PVA – 3 wt% MIL-140 A | 106.36 | 158.37 | 372.26 | 443.14 | 222.54 | 339.55 | 26.70 |

and the dehydration of zirconium atoms [50]. The second decomposition is due to the moisture in the structure of the PVA. The second decomposition temperature was measured at 121°C in the pristine PVA and at 158°C in the PVA – 3 wt% MIL-140 A loaded nanocomposite membrane. Since MIL-140 A has a higher thermal resistance compared to PVA, a positive increase in the second decomposition temperature was observed with the addition of MIL-140 A. Since there was no significant change in the third and fourth decomposition temperatures of the MMM with the addition of MIL-140 A, these degradations are thought to be caused by PVA. Decompositions observed between 370-375°C and 440-445°C occur as a result of the elimination of the acetate groups in the structure of PVA and the main chain decomposition [51, 52]. Additionally, when the residue values were investigated, the amount of residue increased from 20 to 26% with the addition of 3 wt% MIL-140 A. This effect indicates that the MIL-140 A filling causes an enhancement in the thermal durability of PVA. In MMM studies, if ash remains equal to the amount of additive, it means that the additive remains without decomposition throughout the test temperature. With the addition of 3 wt% MIL-140 A, the amount of remaining ash compared to the pristine membrane is around 6% (higher than the amount of filler added to the polymeric matrix), confirming that the membrane increases thermal resistance. Similar effects are also seen in the literature studies [53, 54].

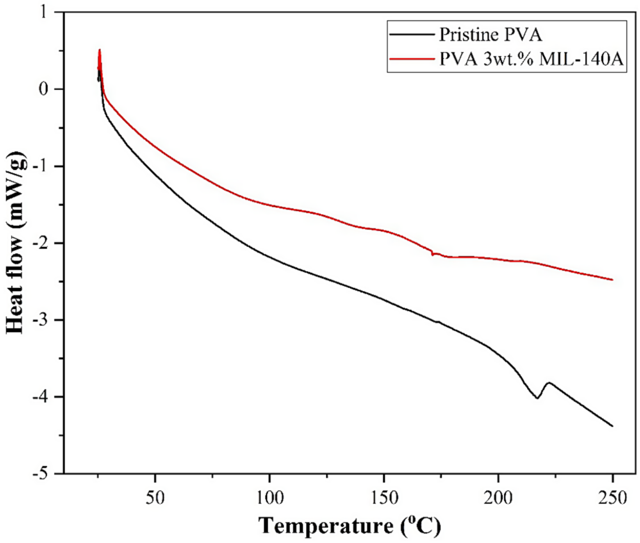

**Fig. 8** DSC thermogram of pristine PVA and PVA – 3 wt% MIL-140 A mixed-matrix membrane

The enthalpy ($\Delta H_m$) and the melting temperature (Tm) of membranes were determined by the DSC and DSC thermograms of pristine PVA and PVA – 3 wt% MIL-140 A membranes are given in Fig. 8. The thermal data ($T_m$ and $\Delta H_m$) of membranes are shown in Table 2. Melting temperatures of the pristine PVA were higher than those of the MIL-140 A loaded membrane. Since the crystal radius of the water molecules present in the structure of PVA has increased in

**Table 2** Thermal properties with DSC

| Samples | $T_{m,\ onset}$ (°C) | $T_{m,\ peak}$ (°C) | $T_{m,\ endset}$ (°C) | $\Delta H_m$ (J/g) |
|---|---|---|---|---|
| Pristine PVA | 205.98 | 216.42 | 220.79 | -35.49 |
| PVA – 3 wt% MIL-140 A | 169.98 | 171.00 | 174.37 | -32.01 |

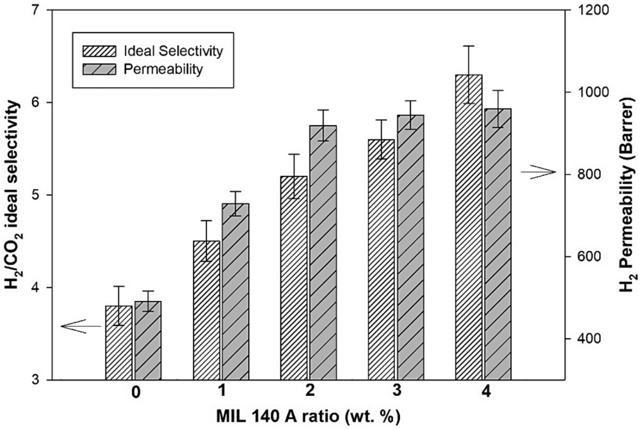

**Fig. 9** Effect of MIL-140 A loading on permeability and selectivity (feed pressure:2 bar)

accordance with the Gibbs-Thomson equation, it has caused the water areas to grow and melting to occur at higher temperatures [55, 56]. With the addition of MIL-140 A, this decrease in melting temperatures can provide a significant advantage in the easy processing of membranes. In addition, it is seen that there is a significant decrease in melting enthalpy with the addition of MIL-140 A. This decrease in melting enthalpy means that less energy is needed, especially to ensure the homogeneous dispersion of nanofillers in the polymeric matrix [57].

The permeability can be enhanced depending on the decrease in the glass transition temperature. The $T_g$ value of the MMM decreased from 78 °C to 71 °C when 3 wt% MIL-140 A was added. This result demonstrates that the MOF incorporation does not restrict segmental mobility and does not have a negative effect on the permeability value.

## 3.2 Gas Separation Results

The gas separation process in polymeric membranes is explained based on the solution-diffusion model. According to this model, gas molecules dissolved on the top surface of the membrane, diffuse through the free voids of the polymeric matrix [58]. In all polymers, the diffusion coefficient decreases with the size of the penetrating molecules; because larger molecules pass through more difficult or slower than smaller molecules [59, 60]. The gas separation performance of membranes is evaluated depending on the permeability and selectivity calculations [61, 62]. Permeability is related to the productivity of the membrane. It is related to the amount of gas separated from the unit area of the membrane per unit time. It is necessary to have high permeability, which is a critical parameter in membrane gas separation studies. Selectivity is as important as the permeability for determining the membrane performance. For an ideal gas separation membrane, both selectivity and permeability should be high. However, a trade-off trend between these two performance parameters can be observed in most studies. Therefore, it is important to overcome this problem by modifications of polymeric membranes.

In this study, gas permeation tests were performed on single gases. Therefore, ideal selectivity values were calculated. The effect of MIL-140 A ratio on the $H_2/CO_2$ selectivity, hydrogen, and carbon dioxide permeability was studied at a constant feed pressure of 2 Bar and room temperature. As seen in Fig. 9, as the MIL-140 A content increased in membrane from zero to 4 wt%, permeability values significantly increased from 491 Barrer to 959 Barrer. Since the MIL-140 A material has a porous structure, the gas diffusion might be accelerated through the molecular diameters of the MOF. While the separation mechanism in non-porous polymers is based on the solution-diffusion model, when porous structures such as MIL-140 A are added into a polymeric matrix, the transition mechanism is based on both the particle transition mechanism (molecular sieve, Knudsen diffusion) and the solution-diffusion model. Therefore, both the pore size and the surface area of filler directly affect the separation performance. Additionally, the additive may change the physical, chemical structure, and crystallinity of the polymeric matrix. In this study, the structure of the PVA polymer has also changed, as seen in XRD, DSC, TGA analyses, and mechanical tests. MIL-140 A changes the structure of the membrane by making it more amorphous and flexible. It was observed from the DSC test that the MIL-140 A incorporation decreased the crystallinity depending on the enthalpy. Moreover, in the mechanical test results, the elongation at break value increased, in other words, the structure became more flexible. This flexibility in the structure also increases inter-chain mobility. Therefore, the increase in gas permeability is a predicted result from the characterization tests.

As shown in the figure, the MIL-140 A contribution increased the selectivity value from 3.8 to 6.3. In studies performed with pure polymeric membranes, increases in permeability generally cause a decrease in selectivity. However, the MIL-140 A additive caused an increase in selectivity as well as permeability. Selectivity in gas permeability depends on diffusion and solution selectivity. The addition of MIL-140 A resulted in increased diffusion selectivity by increasing tortuous pathways by creating transition gaps for hydrogen [63]. According to the surface area measurements made in the previous study, the BET surface area of the MIL-140 A particle was obtained as 388.7 m$^2$/g [42]. This value is quite large and thus the selective voids are distributed within the membrane. Hence, selective gas separation performance improved as expected. Since the kinetic diameter of hydrogen is smaller than carbon dioxide, the selectivity values increased.

In Fig. 10, the effect of pressure on hydrogen/carbon dioxide selectivity and permeability was observed in 3 wt% MIL-140 A loaded nanocomposite membrane. As carbon dioxide is separated through polymeric membranes, some interactions may occur between the carbon dioxide and the polymer. These interactions may cause a change in the structure of the polymer and a change in its selective separation capability. This situation, also known as plasticization, is more effective, especially in gas separation at high pressures. While some polymers may become flexible, their permeability may increase and their selectivity may decrease due to this interaction. The opposite effects may also occur in some polymers.

As seen in Fig. 10, as the feed pressure increased, the permeability value increased. It can be seen that there is no structural degradation in the glassy polymer at low pressures. The increase in the permeability value is attributed to the increase in flux. However, the selectivity value was gradually reduced. This means that the hydrogen permeability of the polymer increases, but the carbon dioxide permeability increases even more, and this is an undesirable situation. In fact, the percentage decrease in selectivity is much higher than the increase in permeability. Therefore, it is possible to conclude that the separation ability of the membrane decreases as the pressure increases.

### 3.3 Comparison of the Study

In this study, for the first time in the literature, MIL 140 A was synthesized and added to the PVA matrix, and its effect on physical, chemical, thermal, mechanical, and separation performance of MMM was determined. Hydrogen and carbon dioxide gas permeation test was performed to determine the ideal selectivity and permeability. Table 3 gives examples of hydrogen purification studies with modified polymers and MOFs.

As can be seen from the table, MOF and ZIF membranes had higher selectivity and permeability values. However, the production costs of these membranes are relatively high compared to polymers. When we compared the separation values in the table where MOFs were used as additives, relatively high values were obtained in this study.

To obtain superior gas separation performance, the permeability/selectivity balance must be well adjusted. The permeability/selectivity balance was defined by Robeson in 1991 and revised by Robeson in 2008. Scientific studies on gas separation aim to approach the upper limit line on the Robeson curve. In Fig. 11, the gas separation results obtained in the present study are given in the Robeson's upper bond-1991 and Robeson's upper bond-2008. The result obtained from the pristine PVA membrane is far from the upper boundary line of the Robeson curves. It is seen that gas separation values approach the Robeson upper limit values with the addition of MIL 140 A. This result is attributed to the MOF material increasing the diffusion selectivity of hydrogen and eliminating the plasticizing effect of carbon dioxide.

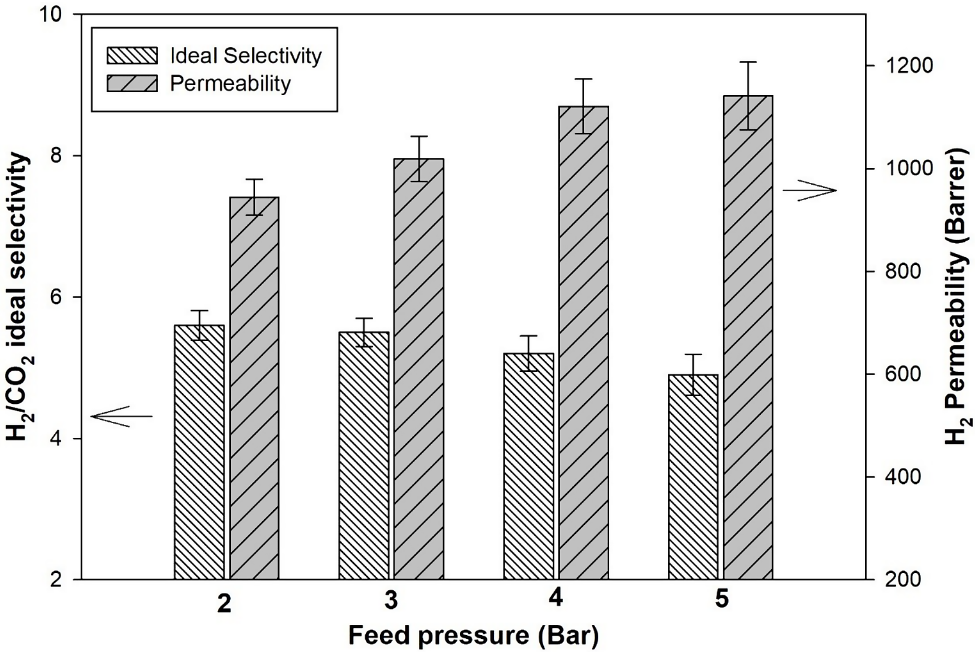

**Fig. 10** Effect of feed pressure on permeability and selectivity (MIL-140 content of 3 wt%)

**Table 3** Comparison of the studies in literature

| Membrane | Feed P(Bar) | Temperature (C) | $H_2/CO_2$ Selectivity | $H_2$ Permeability (Barrer) | Reference |
|---|---|---|---|---|---|
| ZIF 95 | 1 | 325 | 25.7 | > 1*$10^5$ | [64] |
| ZIF-100 | 1 | 25 | 72 | | [65] |
| PBI/ZIF-8 | 30 | 150 | 17 | 65 GPU | [66] |
| Matrimid 5018 | 6 | - | 4.4 | - | [67] |
| SURMOF-Cl | - | 140 | 4.7 | > 2000 | [68] |
| PBI/ZIF-11 | - | 25 | 5.6 | 67.8 | [69] |
| 6FDA-DAM-ZIF-11 | 4 | 30 | 1.06 | 272 | [70] |
| MOF/COF | 1 | 25 | 13.5 | 1.1*$10^5$ | [71] |
| PMMA-NH2-MIL 53 | - | 30 | 53 | 10.94 GPU | [72] |
| PBI | - | 200 | 15 | 45 | [73] |
| PBI/Matrimid(50/50wt.%) | - | 35 | 6.05 | 13 | [74] |
| Polyethyleneimine (CMS) | | 25 | 8.3 | 600 | [75] |
| PVDF-IL | 2 | 30 | 6.67 | 112 | [76] |
| PI + IL | 2 | 35 | 1.2 | 340 | [77] |
| PVA + MIL140A (%4) | 2 | 28 | 6.3 | 959 | This study |
| PVA + MIL140A (%3) | 3 | 28 | 5.5 | 1019 | This study |

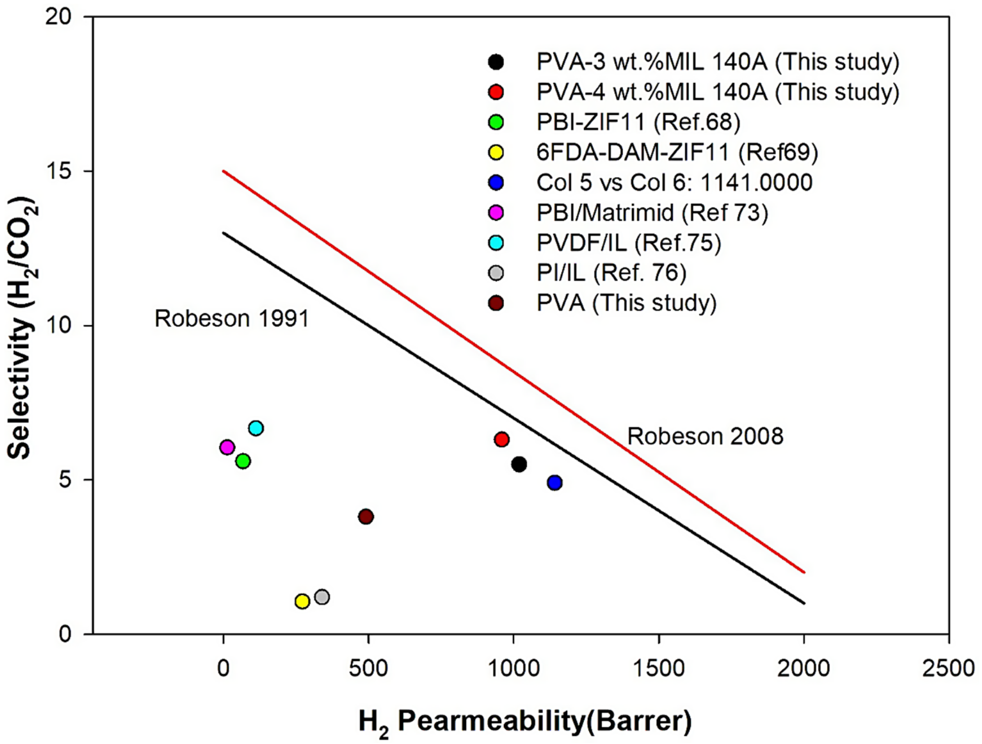

**Fig. 11** Performance of PVA and PVA-MOF mixed matrix membranes in Robeson's upper bound

## 4 Conclusions

In this study, MIL-140 A was added to the PVA matrix for the selective separation of hydrogen. Characterizations and single gas separation tests were performed. According to the results, the membrane was produced in a non-porous manner and the MIL-140 A particles were homogeneously dispersed. The structure of MIL-140 A added membranes became amorphous and the melting enthalpy decreased. MIL-140 A addition significantly increased the mechanical strength from 23.7 MPa to 43.1 MPa up to 3 wt% MIL-140 A incorporation. In gas separation tests, both permeability and selectivity increased as the MIL-140 A ratio increased at 2 bar feed pressure and room conditions. The highest permeability and selectivity were obtained by using 4 wt% of MIL-140 A loaded membrane as 6.3 and 959 Barrer, respectively. Although the selectivity and permeability values increased, the mechanical analysis results showed that overloading (4wt.%) had a negative effect on the mechanical strength. As a result, promising results were obtained with the MIL-140 A loaded PVA nanocomposite membrane.

**Acknowledgements** This study is supported by TÜBİTAK (Project Number :123M086) and the Scientific Research Center of Çanakkale Onsekiz Mart University (Project Number: FBA-2022-4068).

**Author Contributions** Filiz Ugur Nigiz. wrote the main manuscript text, made experimental studyTuba Ünügül prepared figuresAll authors reviewed the manuscript.

**Funding** Open access funding provided by the Scientific and Technological Research Council of Türkiye (TÜBİTAK).

**Data Availability** No datasets were generated or analysed during the current study.

## Declarations

**Competing Interests** The authors declare no competing interests.

## References

1. C.Z. Liang, T.S. Chung, J.Y. Lai, A review of polymeric composite membranes for gas separation and energy production. Prog. Polym. Sci. **97**, 101141 (2019)
2. P. Nikolaidis, A. Poullikkas, A comparative overview of hydrogen production processes. Renew. Sustain. Energy Rev. **67**, 597–611 (2017)
3. F. Dawood, M. Anda, G.M. Shafiullah, Hydrogen production for energy: an overview. Int. J. Hydrog. Energy. **45**(7), 3487–3869 (2020)
4. A.R. Kamble, C.M. Patel, Z.V. Murthy, P. A review on the recent advances in mixed matrix membranes for gas separation processes. Renew. Sustain. Energy Rev. **145**, 111062 (2021)
5. R.S.K. Valappil, N. Ghasem, M. Al-Marzouqi, Current and future trends in polymer membrane-based gas separation technology: a comprehensive review. J. Ind. Eng. Chem. **98**, 103–129 (2021)
6. W.F. Yong, H. Zhang, Recent advances in polymer blend membranes for gas separation and pervaporation. Prog. Mater. Sci. **116**, 100713 (2021)
7. C.R. Bilchak, M. Jhalaria, Y. Huang, Z. Abbas, J. Midya, F.M. Benedetti, S.K. Kumar, Tuning selectivities in gas separation membranes based on polymer-grafted nanoparticles. ACS Nano. **14**(12), 17174–17183 (2020)
8. R. Castro-Muñoz, K.V. Agrawal, J. Coronas, Ultrathin permselective membranes: the latent way for efficient gas separation. RSC Adv. **10**(21), 12653–12670 (2020)
9. M. Farnam, bin H. Mukhtar, bin, A. Mohd Shariff, A review on glassy and rubbery polymeric membranes for natural gas purification. ChemBioEng Reviews. 2021;8(2):90–109
10. C.Y. Liang, P. Uchytil, R. Petrychkovych, Y.C. Lai, K. Friess, M. Sipek, S.Y. Suen, A comparison on gas separation between PES (polyethersulfone)/MMT (Na-montmorillonite) and PES/TiO2 mixed matrix membranes. Sep. Purif. Technol. **92**, 57–63 (2012)
11. X. Gao, Z.K. Li, J. Xue, Y. Qian, L.Z. Zhang, J. Caro, H. Wang, Titanium carbide Ti3C2Tx (MXene) enhanced PAN nanofiber membrane for air purification. J. Membr. Sci. **586**, 162–169 (2019)
12. S.S. Karim, A. Hussain, S. Farrukh, M. Younas, Effects of coagulation residence time on the morphology and properties of poly (vinyl) alcohol (PVA) asymmetric membrane via NIPS method for O2/N2 separation. J. Polym. Environ. **28**, 2810–2822 (2020)
13. S. Tourani, F. Akbarbandari, Investigation of the gas separation properties of polyurethane membranes in Presence of Boehmite Nanoparticles. J. Inorg. Organomet. Polym Mater. **33**(1), 61–75 (2023)
14. M. Mosadegh, F. Amirkhani, H.R. Harami, M. Asghari, M.J. Parnian, Effect of Nafion and APTEOS functionalization on mixed gas separation of PEBA-FAU membranes: experimental study and MD and GCMC simulations. Sep. Purif. Technol. **247**, 116981 (2020)
15. Q. Cao, X. Ding, H. Zhao, L. Zhang, Q. Xin, Y. Zhang, Improving gas permeation performance of PDMS by incorporating hollow polyimide nanoparticles with microporous shells and preparing defect-free composite membranes for gas separation. J. Membr. Sci., 2021:635; 119508
16. S. Aruldass, V. Mathivanan, A.R. Mohamed, C.T. Tye, Factors affecting hydrolysis of polyvinyl acetate to polyvinyl alcohol. J. Environ. Chem. Eng. (2019). https://doi.org/10.1016/j.jece.2019.103238
17. D. Yadav, A. Karunanithi, S. Saxena, S. Shukla, Modified PVA membrane for separation of micro-emulsion. Sci. Total Environ. **822**, 153610 (2022)
18. M. Mokarinezhad, S.S. Hosseini, S.A. Ghadimi, E. Asadi, Assessment of the effect of modification of ZIF-8 nanoparticles by the CTAB Cationic surfactant on the performance of ZIF-8/PVA mixed matrix membranes in Pervaporation Dehydration of Isopropanol. Nashrieh Shimi va. Mohandesi Shimi Iran. **42**(2), 247–260 (2023)
19. E.F. Mohamed, F. Mohamed, A. El-Mekawy, E. Hotaby, Development of PVA/GO nanocomposites membranes for air-filtration and purification. J. Inorg. Organomet. Polym Mater. **33**(11), 3389–3401 (2023)
20. Y. Zhao, H. Tian, Y. Ouyang, A. Xiang, X. Luo, X. Shi, S. Ma, Poly (Vinyl Alcohol) Composite membrane with polyamidoamine dendrimers for efficient separation of CO2/H2 and CO2/N2. J. Polym. Environ. **30**(10), 4193–4200 (2022)
21. A. Raza, S. Farrukh, A. Hussain, Synthesis, characterization and NH3/N2 gas permeation study of nanocomposite membranes. J. Polym. Environ. **25**, 46–55 (2017)
22. W. Xu, A. Lindbråthen, S. Janakiram, L. Ansaloni, L. Deng, Enhanced CO2/H2 separation by GO and PVA-GO embedded PVAm nanocomposite membranes. J. Membr. Sci. **671**, 121397 (2023)
23. M. Klepić, K. Setničková, M. Lanč, Permeation and sorption properties of CO2-selective blend membranes based on polyvinyl alcohol (PVA) and 1-ethyl-3-methylimidazolium dicyanamide ([EMIM][DCA]) ionic liquid for effective CO2/H2 separation. J. Membr. Sci. (2020). https://doi.org/10.1016/j.memsci.2019.117623
24. K.C. Wong, P.S. Goh, A.F. Ismail, Enhancing hydrogen gas separation performance of thin film composite membrane through facilely blended polyvinyl alcohol and PEBAX. Int. J. Hydrog. Energy. **46**, 19737–19748 (2021)
25. D.F. Sanders, Z.P. Smith, R. Guo, L.M. Robeson, J.E. McGrath, D.R. Paul, B.D. Freeman, Energy-efficient polymeric gas

separation membranes for a sustainable future: a review. Polymer. **54**(18), 4729–4761 (2013)

26. R. Xing, W.S.W. Ho, Crosslinked polyvinylalcohol–polysiloxane/fumed silica mixed matrix membranes containing amines for CO2/H2 separation. J. Membr. Sci. **367**(1–2), 91–102 (2011)
27. J. Ahmad, K. Deshmukh, M.B. Hägg, Influence of TiO2 on the chemical, mechanical, and gas separation properties of polyvinyl alcohol-titanium dioxide (PVA-TiO2) nanocomposite membranes. Int. J. Polym. Anal. Charact. **18**(4), 287–296 (2013)
28. M. Kheirtalab, R. Abedini, M. Ghorbani, A novel ternary mixed matrix membrane comprising polyvinyl alcohol (PVA)-modified poly (ether-block-amide)(Pebax®1657)/graphene oxide nanoparticles for CO2 separation process Safety and Environmental. Protection. **144**, 208–224 (2020)
29. X. Li, M. Guo, P. Bandyopadhyay, Q. Lan, H. Xie, G. Liu, J.H. Lee, Two-dimensional materials modified layered double hydroxides: a series of fillers for improving gas barrier and permselectivity of poly(vinyl alcohol). Compos. Part. B: Eng., 2021;207;108568.
30. A. Imtiyaz, A.A. Singh, Study of the fabrication of different-dimensional metal–Organic frameworks and their hybrid composites for Novel Applications. J. Inorg. Organomet. Polym Mater. **33**(10), 3027–3048 (2023)
31. Y.Z. Li, G.D. Wang, L.N. Ma, L. Hou, Y.Y. Wang, Z. Zhu, Multiple functions of gas separation and vapor adsorption in a new MOF with open tubular channels. ACS Appl. Mater. Interfaces. **13**(3), 4102–4109 (2021)
32. H. Daglar, S. Aydin, S. Keskin, MOF-based MMMs breaking the upper bounds of polymers for a large variety of gas separations. Sep. Purif. Technol. **281**, 119811 (2022)
33. N. Koralkar, S. Mehta, A. Upadhyay, G. Patel, K. Deshmukh, MOF-Based nanoarchitectonics for Lithium-ion batteries: a Comprehensive Review. J. Inorg. Organomet. Polym Mater., 2023;1–27
34. Y. Cheng, S.J. Datta, S. Zhou, J. Jia, O. Shekhah, M. Eddaoudi, Advances in metal–organic framework-based membranes. Chem. Soc. Rev. **51**(19), 8300–8350 (2022)
35. A. Felix Sahayaraj, H. Joy Prabu, J. Maniraj, M. Kannan, M. Bharathi, P. Diwahar, J. Salamon, Metal–organic frameworks (MOFs): the next generation of materials for catalysis, gas storage, and separation. J. Inorg. Organomet. Polym Mater. **33**(7), 1757–1781 (2023)
36. S. Yu, H. Pang, S. Huang, H. Tang, S. Wang, M. Qiu, X. Wang, Recent advances in metal-organic framework membranes for water treatment: a review. Sci. Total Environ. **800**, 149662 (2021)
37. C. Vieira Soares, D. Borges, D. Wiersum, Adsorption of small molecules in the porous zirconium-based metal organic framework MIL-140A (zr): a joint computational-experimental approach. J. Phys. Chem. C **120**, 7192–7200 (2016)
38. A.H. Ozen, B. Ozturk, Gas separation characteristic of mixed matrix membrane prepared by MOF-5 including different metals. Sep. Purif. Technol. **211**, 514–521 (2019)
39. S. Ashtiani, M. Khoshnamvand, C. Regmi, K. Friess, Interfacial design of mixed matrix membranes via grafting PVA on UiO-66-NH2 to enhance the gas separation performance. Membranes. **11**(6), 419 (2021)
40. M. Prakash, H. Jobic, N.A. Ramsahye, F. Nouar, D. Damasceno Borges, C. Serre, G. Maurin, Diffusion of H2, CO2, and their mixtures in the porous zirconium based metal-organic framework MIL-140A(zr): combination of quasi-elastic neutron scattering measurements and molecular dynamics simulations. J. Phys. Chem. **119**, 23978–23989 (2015)
41. G. Yang, Z. Xie, M. Cran, D. Ng, S. Gray, Enhanced desalination performance of poly (vinyl alcohol)/carbon nanotube composite pervaporation membranes via interfacial engineering. J. Membr. Sci. **579**, 40–51 (2019)
42. F.U. Nigiz, B. Karakoca, Pervaporative desalination using MIL-140A loaded polylactic acid nanocomposite membrane. Process Saf. Environ. Prot. **169**, 447–457 (2023)
43. N.Z.S. Yahaya, S.H. Paiman, N. Abdullah, N. Mu'ammar Mahpoz, A.A. Raffi, M.A. Rahman, J. Jaafar, Synthesis and characterizations of MIL-140B-Al2O3/YSZ ceramic membrane using solvothermal method for seawater desalination. J. Aust. Ceram. Soc. **56**(1), 291–300 (2020)
44. T. Ünügül, F.U. Nigiz, Hydrogen purification using natural zeolite-loaded hydroxyethyl cellulose membrane. Int. J. Energy Res. (2021). https://doi.org/10.1002/er.7299
45. X. Xu, Y.Q. Yang, Y.Y. Xing, J.-F. Yang, S.F. Wang, Properties of novel polyvinyl alcohol/cellulose nanocrystals/silver nanoparticles blend membranes. Carbohydr. Polym. **98**(2), 1573–1577 (2013)
46. A. Abdolmaleki, S. Mallakpour, S. Borandeh, Improving interfacial interaction ofl-phenylalanine-functionalized graphene nanofiller and poly(vinyl alcohol) nanocomposites for obtaining significant membrane properties: morphology, thermal, and mechanical studies. Polym. Compos. **37**(6), 1924–1935 (2015)
47. A. Abdolmaleki, S. Mallakpour, A. Karshenas, Synthesis and characterization of new nanocomposites films using alanine-Cu-functionalized graphene oxide as nanofiller and PVA as polymeric matrix for improving of their properties. J. Solid State Chem. **253**, 398–405 (2017)
48. Jodłowski, P.J., Kurowski, G., Dymek, K., Oszajca, M., Piskorz, W., Hyjek, K., ... & Sitarz, M. From crystal phase mixture to pure metal-organic frameworks–Tuning pore and structure properties. Ultrasonics Sonochemistry, 2023;95, 106377.
49. W. Liang, R. Babarao, D.M. D'Alessandro, Microwave-assisted solvothermal synthesis and optical properties of tagged MIL-140A metal–organic frameworks. Inorg. Chem. **52**(22), 12878–12880 (2013)
50. C. Healy, K.M. Patil, B.H. Wilson, L. Hermanspahn, N.C. Harvey-Reid, B.I. Howard, C. Kleinjan, J.D. Holladay, J. Hu, D.L. King, Y. Wang, An overview of hydrogen production technologies. Catal. Today. **139**(4), 244–260 (2009)
51. Q. Ma, L. Du, Y. Yang, L. Wang, Rheology of film-forming solutions and physical properties of tara gum film reinforced with polyvinyl alcohol (PVA). Food Hydrocoll. **63**, 677–684 (2017)
52. B. Ucpinar Durmaz, A. Aytac, Effects of polyol-based plasticizer types and concentration on the properties of polyvinyl alcohol and casein blend films. J. Polym. Environ. **29**(1), 313–322 (2020)
53. H. Wang, H. Qiao, J. Guo, J. Sun, H. Li, S. Zhang, X. Gu, Preparation of cobalt-based metal organic framework and its application as synergistic flame retardant in thermoplastic polyurethane (TPU). Compos. Part. B: Eng. (2019). https://doi.org/10.1016/j.compositesb.2019.107498
54. N.A. Khan, M.B.K. Niazi, F. Sher, Z. Jahan, T. Noor, O. Azhar, T. Rashid, Iqbal, N. Metal Organic Frameworks Derived Sustainable Polyvinyl Alcohol/Starch Nanocomposite Films as Robust materials for packaging applications. Polymers. (2021). https://doi.org/10.3390/polym13142307
55. C.L. Jackson, G.B. McKenna, The melting behavior of organic materials confined in porous solids. J. Chem. Phys. **93**(12), 9002–9011 (1990)
56. B.-J. Hwang, J. Joseph, Y.-Z. Zeng, C.-W. Lin, M.-Y. Cheng, Analysis of states of water in poly (vinyl alcohol) based DMFC membranes using FTIR and DSC. J. Membr. Sci. **369**(1–2), 88–95 (2011)
57. G. Guerrero, M.B. Hägg, C. Simon, T. Peters, N. Rival, C. Denonville, CO2 separation in nanocomposite membranes by the addition of amidine and lactamide functionalized POSS® nanoparticles into a PVA layer. Membr. (Basel). (2018). https://doi.org/10.3390/membranes8020028

58. Y. Han, W.W. Ho, Polymeric membranes for CO2 separation and capture. J. Membr. Sci. **628**, 119244 (2021)
59. M.L. Jue, R.P. Lively, Targeted gas separations through polymer membrane functionalization. Reactive Funct. Polym. **86**, 88–110 (2015)
60. R. Bounaceur, E. Berger, M. Pfister, A.A. Ramirez Santos, E. Favre, Rigorous variable permeability modelling and process simulation for the design of polymeric membrane gas separation units: MEMSIC simulation tool. J. Membr. Sci. **523**, 77–91 (2017)
61. H.A. Mannan, H. Mukhtar, T. Murugesan, R. Nasir, D.F. Mohshim, A. Mushtaq, Recent applications of polymer blends in gas separation membranes. Chem. Eng. Technol. **36**(11), 1838–1846 (2013)
62. S. Khoonsap, S. Rugmai, W.-S. Hung, K.-R. Lee, S. Klinsrisuk, S. Amnuaypanich, Promoting permeability-selectivity anti-trade-off behavior in polyvinyl alcohol (PVA) nanocomposite membranes. J. Membr. Sci. **544**, 287–296 (2017)
63. Ahmad, N. N. R., Yang, L., Hamid, M. R. A., Ghazi, T. I. M., Nasir, R., Leo, C. P., ... & Tiong, S. K. (2023). Unlocking the Potential of Metal-Organic Frameworks-Based Mixed Matrix Membranes for Hydrogen Separation and Purification. Journal of Industrial and Engineering Chemistry.
64. A. Huang, Y. Chen, N. Wang, Z. Hu, J. Jiang, J. Caro, A highly permeable and selective zeolitic imidazolate framework ZIF-95 membrane for H2/CO2 separation. Chem. Commun. **48**(89), 10981–10983 (2012)
65. N. Wang, Y. Liu, Z. Qiao, L. Diestel, J. Zhou, A. Huang, J. Caro, Polydopamine-based synthesis of a zeolite imidazolate framework ZIF-100 membrane with high H2/CO2 selectivity. J. Mater. Chem. A **3**(8), 4722–4728 (2015)
66. Etxeberria-Benavides, M., Johnson, T., Cao, S., Zornoza, B., Coronas, J., Sanchez-Lainez, J., ... & David, O. PBI mixed matrix hollow fiber membrane: Influence of ZIF-8 filler over H2/CO2 separation performance at high temperature and pressure. Separation and Purification Technology, 2020;237, 116347.
67. O.C. David, D. Gorri, A. Urtiaga, I. Ortiz, Mixed gas separation study for the hydrogen recovery from H2/CO/N2/CO2 post combustion mixtures using a Matrimid membrane. J. Membr. Sci. **378**(1–2), 359–368 (2011)
68. Journal of Materials Chemistry A, 2023;11(45), 24724–24737
69. L. Li, J. Yao, X. Wang, Y.B. Cheng, H. Wang, ZIF-11/Polybenzimidazole composite membrane with improved hydrogen separation performance. J. Appl. Polym. Sci., 2014;**131**(22)
70. M.S. Boroglu, A.B. Yumru, Gas separation performance of 6FDA-DAM-ZIF-11 mixed-matrix membranes for H2/CH4 and CO2/CH4 separation. Sep. Purif. Technol. **173**, 269–279 (2017)
71. J. Fu, S. Das, G. Xing, T. Ben, V. Valtchev, S. Qiu, Fabrication of COF-MOF composite membranes and their highly selective separation of H2/CO2. J. Am. Chem. Soc. **138**(24), 7673–7680 (2016)
72. Y. Zhao, D. Zhao, C. Kong, F. Zhou, T. Jiang, L. Chen, Design of thin and tubular MOFs-polymer mixed matrix membranes for highly selective separation of H2 and CO2. Sep. Purif. Technol. **220**, 197–205 (2019)
73. L. Zhu, M.T. Swihart, H. Lin, Tightening polybenzimidazole (PBI) nanostructure via chemical cross-linking for membrane H2/CO2 separation. J. Mater. Chem. A **5**(37), 19914–19923 (2017)
74. S.S. Hosseini, T.S. Chung, Carbon membranes from blends of PBI and polyimides for N2/CH4 and CO2/CH4 separation and hydrogen purification. J. Membr. Sci. **328**(1–2), 174–185 (2009)
75. H.H. Tseng, C.T. Wang, G.L. Zhuang, P. Uchytil, J. Reznickova, K. Setnickova, Enhanced H2/CH4 and H2/CO2 separation by carbon molecular sieve membrane coated on titania modified alumina support: effects of TiO2 intermediate layer preparation variables on interfacial adhesion. J. Membr. Sci. **510**, 391–404 (2016)
76. P. Cserjési, N. Nemestóthy, K. Bélafi-Bakó, Gas separation properties of supported liquid membranes prepared with unconventional ionic liquids. J. Membr. Sci. **349**(1–2), 6–11 (2010)
77. S. Kanehashi, M. Kishida, T. Kidesaki, R. Shindo, S. Sato, T. Miyakoshi, K. Nagai, CO2 separation properties of a glassy aromatic polyimide composite membranes containing high-content 1-butyl-3-methylimidazolium bis (trifluoromethylsulfonyl) imide ionic liquid. J. Membr. Sci. **430**, 211–222 (2013)